

Exact many-body scars based on pairs or multimers in a chain of spinless fermions

Lorenzo Gotta,^{1,*} Leonardo Mazza,¹ Pascal Simon,² and Guillaume Roux¹

¹*Université Paris-Saclay, CNRS, LPTMS, 91405, Orsay, France.*

²*Université Paris-Saclay, CNRS, Laboratoire de Physiques des Solides, 91405, Orsay, France.*

(Dated: September 5, 2022)

We construct a 1D model Hamiltonian of spinless fermions for which the spinless analogue of η -pairing states are quantum many-body scars of the model. These states are excited states and display subvolume entanglement entropy scaling; they form a tower of states that are equally spaced in energy (resulting in periodic oscillations in the Loschmidt echo and in the time evolution of observables for initial states prepared in a superposition of them) and are atypical in the sense that they weakly break the eigenstate thermalization hypothesis, while the other excited states are thermal. We conclude by presenting models with a tower of scar states generated by multimers located at the edge of the Brillouin zone.

I. INTRODUCTION

The question of thermalization in isolated many-body quantum systems typically relies on the eigenstate-thermalization-hypothesis (ETH) [1–4], which assumes that highly-excited eigenstates of nonintegrable quantum many-body systems act as effective baths for their small subsystems, thus allowing a conventional statistical ensemble description of local observables. An active research area stemming from the introduction of ETH has been the search for systems that violate such a conjecture and hence display anomalous thermalization behavior.

The strategies towards the realization of systems lacking standard thermalization under unitary time evolution have relied on the presence of an extensive number of integrals of motion, thereby enforcing the time-evolved state to retain memory of its initial configuration. The two representatives of the aforesaid routes towards ETH-breaking are fine-tuned integrable systems, featuring an extensive set of global conserved quantities [5–12], and strongly disordered systems, where the phenomenon of many-body-localization has been explained by introducing the idea of local integrals of motion [13–21].

More recently, an experiment on quantum quenches in a system of cold Rydberg atoms revealed persistent coherent oscillations in local observables when monitoring the time evolution starting from a specific initial state [22]. Such a feature was shown to rely on the presence of a measure-zero set of exceptional ETH-violating eigenstates, called quantum many-body scars [23–26], embedded in an otherwise thermalizing spectrum [27–31]. A recent observation of many-body scarring in a quantum simulator has also been reported [32–34]. The latter have been later constructed in several nonintegrable models of spin-1 [30, 35–40] and spin- $\frac{1}{2}$ chains [39–42] or, more generically, spin- S chains [43], as well as in spinful fermionic systems in one and higher dimensions [44–46] and in quantum Hall models [47]. They all have the form of energetically equally-spaced towers of exact eigenstates of the Hamiltonian, and this peculiar spectral feature lies at the hearth of the observed periodic revivals in the time evolution of suitably chosen local observables. Further examples of

quantum many-body scars have been predicted in the framework of Floquet-engineered systems [48–51], lattice gauge theories [52–54], flat-band models [55, 56] and magnetically-frustrated systems [55, 57, 58].

A crucial step towards the understanding of quantum many-body scars was played by η -pairing states, firstly discovered by Yang as exact excited eigenstates of the Hubbard model with off-diagonal long-range order [59]. Despite the η -pairing states not representing genuine many-body scars of the Hubbard model due to the presence of a hidden η -pairing $SU(2)$ symmetry, they display the prototypical algebraic properties of towers of scarred eigenstates, as they are generated by the repeated application of a ladder-like operator to a weakly-entangled state, and a subvolume entanglement entropy scaling law [60]. Thus, the η -pairing states have inspired several works aiming at unveiling a universal scarring mechanism allowing for the microscopic emergence of many-body scars, as well as the search for Hubbard-like Hamiltonians with η -pairing-symmetry-breaking terms that preserve analytically tractable towers of η -pairing states as genuine many-body scars [44].

In this work, we unveil the existence of an exact tower of scarred eigenstates of a spinless fermion Hamiltonian by generalizing the mechanism of η -pairing to the case of spinless fermions. Our analysis provides a further illustration of the characteristic properties of towers of scarred eigenstates studied in the literature. The scarred eigenstates are characterized by ETH-violating properties such as the logarithmic scaling of the entanglement entropy in the size of the selected subsystem [27, 29, 38, 41, 44, 60, 61] and the off-diagonal long-range order [41, 61–64] in the pair correlation function. Moreover, we show how the choice of a superposition of scarred eigenstates as the initial state of the time evolution leads to periodic revivals in the expectation values of local observables [41, 61, 65]. We highlight the peculiar feature of symmetry enhancement in the scarred subspace by drawing connections to the concept of quasi-symmetry [66, 67] and its relation to many-body scar dynamics. Remarkably, all these results can be extended to scar states characterised by multimers where $M > 2$ particles are bound together; we discuss explicitly the case $M = 3$, where trimers are fermionic and display some qualitative different features with respect to the bosonic case.

* lorenzo.gotta@universite-paris-saclay.fr

Despite the aforementioned phenomenology being known, we wish to highlight the aspects of our work that have not been significantly underlined in the preceding literature. Firstly, we extend pioneering results on many-body scars in spinful fermionic systems, where η -pairs represent the infinitely long-lived quasiparticles that underlie the corresponding tower of scarred eigenstates [44]. More precisely, we reveal how an analogous structure is realized in a system of spinless fermions. The extended spatial structure of the quasiparticles, namely pairs or multimers of spinless fermions, reflects itself into nonlocal expressions for the lowering operator in the scarred subspace (also discussed in Ref. [41]) and for a nontrivial conserved quantity of the many-body scar dynamics. Moreover, we highlight the fact that our paired scarred states can be interpreted within the framework of macroscopic quantum coherence in the grand-canonical ensemble by constructing a close analogue of bosonic coherent states [43]. Our result differs from the one expected in the case of a purely bosonic mode as a result of the hard-core nature of the pairs. The fermionic case is even more peculiar: although we are able to write the scarred states analytically and to identify them in numerical simulations, we were not able to find an expression for the raising and lowering operators that is local. To the best of our knowledge, so far at least one of the two has always been found.

This article is organised as follows. The first part of the article is devoted to scars based on pairs; in Section II, we introduce the model Hamiltonian and discuss the structure of the interaction term. Section III is then devoted to the definition of the tower of scarred eigenstates and to the detailed analytical characterization of their spectral and entanglement properties, thereby underlining their consequences on the dynamics. Our analysis is corroborated in Section IV with the presentation of some numerical data. The second part of the article consists in Section V, where we extend our results to the multimer case: we present a simple Hamiltonian that supports exact multimer scars and we briefly argue with analytical and numerical results that the model is not integrable and that the scars are not generic. The conclusions are presented in Sec. VI.

II. THE MODEL

We start our discussion focusing on a model that features exact many-body scar states that generalise η -pairing to a spinless fermion chain:

$$\begin{aligned} \hat{H} = & -t \sum_j \left[\hat{c}_j^\dagger \hat{c}_{j+1} + H.c. \right] - J \sum_j \left[\hat{c}_j^\dagger \hat{n}_{j+1} \hat{c}_{j+2} + H.c. \right] + \\ & -\mu \sum_j \hat{n}_j + J \sum_j \left[\hat{n}_{j+1} (\hat{n}_j + \hat{n}_{j+2}) - 2\hat{n}_j \hat{n}_{j+1} \hat{n}_{j+2} \right]; \end{aligned} \quad (1)$$

the fermionic creation and annihilation operators satisfy the canonical anticommutation relations $\{c_i, c_j\} = 0$ and $\{\hat{c}_i, \hat{c}_j^\dagger\} = \delta_{i,j}$. The hopping amplitude is t , μ is the chemical potential and J is the pair-hopping amplitude, associated

to the motion of two neighboring particles; J is also the parameter of different forms of density-density interactions. We take $J > 0$ and $t > 0$. This kind of correlated pair-hopping has been recently studied in a variety of works and is responsible for several phenomena related to pairing [68–73]. The Hamiltonian commutes with the total number of particle operator $\hat{N} = \sum_j \hat{n}_j$. Through this article, for simplicity, we always assume L and N to be even and we take open boundary conditions if not explicitly mentioned. To ease readability, we write explicitly the bounds of summation only when they are non-trivial.

III. EXACT RESULTS AND TOWERS OF STATES

We now discuss a set of scarred eigenstates for \hat{H} . In order to do so, we define the tower of states for $k \in \{0, 1, \dots, L/2\}$:

$$|\psi_{k,\pi}\rangle = \frac{1}{\sqrt{\binom{L-k}{k}}} \frac{(\hat{\eta}_\pi^\dagger)^k}{k!} |0\rangle, \quad \text{with } \hat{\eta}_\pi^\dagger = \sum_j (-1)^j \hat{c}_j^\dagger \hat{c}_{j+1}^\dagger. \quad (2)$$

This set of states is the closest analogue of η -pairing in a spinless fermionic setup as they represent a condensate of pairs at the edge of the first Brillouin zone with fixed number of pairs k (and thus number of fermions $N = 2k$).

The normalization factor follows from combinatorial considerations. Indeed, given N fermions on a lattice of size L , one can map each fermionic configuration where particles form even-sized clusters to a spin configuration with k spin-up states on a spin chain of size $L - k$ via the rules $|\bullet\bullet\rangle \rightarrow |\uparrow\rangle, |\circ\rangle \rightarrow |\downarrow\rangle$. Then, the number of fully-paired fermionic configurations on the original lattice equals the number of ways of distributing k spins-up on a chain of length $L - k$, which is $\binom{L-k}{k}$.

The states introduced in Eq. (2) form a tower of energetically equally-spaced eigenstates of \hat{H} , satisfying the eigenvalue equation:

$$\hat{H} |\psi_{k,\pi}\rangle = -2\mu k |\psi_{k,\pi}\rangle. \quad (3)$$

This result is explicitly derived in Appendix A; very briefly, it follows from the destructive interference of the single fermions when single-particle hopping breaks a pair into two fermions (similar mechanisms have been also highlighted in other models, e.g. spin-1 models [28]).

Moreover, the $|\psi_{k,\pi}\rangle$ satisfy the standard restricted spectrum-generating algebra (RSGA) typical of the tower of states:

$$[\hat{H}, \hat{\eta}_\pi^\dagger] |\psi_{k,\pi}\rangle = -2\mu \hat{\eta}_\pi^\dagger |\psi_{k,\pi}\rangle, \quad (4)$$

and as such they fit exactly in the standard theory of exact many-body scars with linearly-separated energies. Additionally, the states $|\psi_{k,\pi}\rangle$ are the exact frustration-free ground states of the Hamiltonian $\hat{H}_J = +(J/2) \sum_j L_j^\dagger L_j$ for $J > 0$, where

$$\hat{L}_j = \hat{n}_j \hat{n}_{j+1} - \hat{n}_{j+1} \hat{n}_{j+2} + \hat{c}_{j+2}^\dagger \hat{n}_{j+1} \hat{c}_j - \hat{c}_j^\dagger \hat{n}_{j+1} \hat{c}_{j+2}, \quad (5)$$

which corresponds to the part proportional to J of the model in Eq. (1). Thus, we can interpret them as scars obtained by deforming a frustration-free non-integrable model, the deformation being obtained by adding the single-particle hopping and the chemical potential.

The fact that pairs located at momentum π are eigenstates of the Hamiltonian means that they can be thought of as quasi-particles with infinite lifetime; the equal energy spacing is instead associated to the fact that they are not interacting (see Appendix B for a coordinate Bethe Ansatz argument supporting the latter observation). It is enough to assume $t \gg |\mu|$ to place them in the middle of the spectrum of \hat{H} , of which they become exact eigenstates that lie at an extensive energy above the ground-state one.

It is not difficult to observe that the $|\psi_{k,\pi}\rangle$ feature off-diagonal long-range order; let us introduce:

$$P_k(r) = \langle \psi_{k,\pi} | \hat{c}_j^\dagger \hat{c}_{j+1}^\dagger \hat{c}_{j+r} \hat{c}_{j+r+1} | \psi_{k,\pi} \rangle, \quad (6)$$

to denote the pair correlation function evaluated on the state $|\psi_{k,\pi}\rangle$. Then, taking periodic boundary conditions and the thermodynamic limit at fixed density $n = 2k/L$, we obtain

$$\lim_{L \rightarrow \infty} P_k(r) = (-1)^{r+1} \frac{n}{2-n} (1-n)^2, \quad (7)$$

with $r > 3$. The explicit formula at finite size is given in Appendix C. This observation alone is sufficient to motivate the fact that they are exceptional in the spectrum of the Hamiltonian, as they violate the Mermin-Wagner theorem about thermal states in one dimension. As a further proof, we will later also discuss the fact that the entanglement entropy of these states grows logarithmically with the subsystem length, instead of linearly, as it is typically expected for thermal states.

A. Algebraic properties

As mentioned, the operators $\hat{\eta}_\pi^\dagger$ realise a RSGA in the subspace \mathcal{S} spanned by the $|\psi_{k,\pi}\rangle$. Indeed, the commutator $[\hat{H}, \hat{\eta}_\pi^\dagger]$ reads:

$$[\hat{H}, \hat{\eta}_\pi^\dagger] = -2\mu\hat{\eta}_\pi^\dagger + \hat{O}, \quad (8)$$

where the explicit expression for \hat{O} is given in Appendix D. There, we also show that the states $|\psi_{k,\pi}\rangle$ belong to the kernel of \hat{O} . Therefore, Eq. (4) is satisfied and, in turn, the eigenvalue equation (3) is proven in a way that is different from that presented in Appendix A.

More interestingly, we observe peculiar consequences of the spatial structure of the pairs when considering a lowering operator $\hat{\eta}'_\pi$ satisfying $\hat{\eta}'_\pi |\psi_{k,\pi}\rangle \propto |\psi_{k-1,\pi}\rangle$ for $k \geq 1$ and $\hat{\eta}'_\pi |\psi_{k=0,\pi}\rangle = 0$. The naive guess $\hat{\eta}'_\pi = \hat{\eta}_\pi$ fails, as one can notice by studying the explicit case $k = 2, L = 4$:

$$\hat{\eta}_\pi |\psi_{2,\pi}\rangle = \hat{\eta}_\pi |\bullet \bullet \bullet \bullet\rangle = |\bullet \circ \bullet \bullet\rangle - |\circ \bullet \bullet \bullet\rangle - |\bullet \bullet \circ \bullet\rangle, \quad (9)$$

where the filled dots indicate occupied sites, while empty dots denote empty sites. As one can infer from Eq. (9), the action of $\hat{\eta}_\pi$ on $|\psi_{k,\pi}\rangle$ generates configurations with unpaired

fermions as soon as $k > 1$, thus failing to reproduce the properties of a lowering operator inside the subspace \mathcal{S} .

In general, the explicit form of $\hat{\eta}'_\pi$ is rather complicated, we discuss here below for simplicity an expression that works if applied on states $|\psi_{k,\pi}\rangle$ for $k < L/3$, and that is non-local:

$$\hat{\eta}'_\pi = \sum_{\ell=1}^{L-1} \frac{1}{\ell} \sum_{m=0}^{L-1} \frac{e^{2\pi i \frac{m(\ell-\hat{C})}{L}}}{L} \sum_{j=1}^{L-1} e^{-i\pi j} \hat{P}^{(j-1)} \hat{c}_{j+1} \hat{c}_j. \quad (10)$$

In Eq. (10), the operator $\hat{C} = \sum_{j=1}^{L-1} (1-\hat{n}_j)(1-\hat{n}_{j+1})$ counts the number of consecutive sites that are empty and the sum over m represents a Kronecker delta that selects the value of ℓ that is equal to the eigenvalue of the operator \hat{C} . The two operators $\hat{c}_{j+1} \hat{c}_j$ annihilate a pair at sites j and $j+1$ and the projectors $\hat{P}^{(j-1)}$ check that the site j is preceded by an even number of occupied sites and otherwise they annihilate the Fock state. Comparing with the sketch in Eq. (9), this term has the goal of avoiding that the unpaired configuration $|\bullet \circ \bullet \bullet\rangle$ is generated from the initial state $|\bullet \bullet \bullet \bullet\rangle$. It is possibly interesting to observe that there is a recursion relation obeyed by the projectors:

$$\begin{aligned} \hat{P}^{(0)} &= 1, \\ \hat{P}^{(s)} &= 1 - \hat{n}_s \hat{P}^{(s-1)}, \quad 1 \leq s \leq L. \end{aligned} \quad (11)$$

We claim that $\hat{\eta}'_\pi |\psi_k\rangle \propto |\psi_{k-1,\pi}\rangle$. Indeed, if one can show that each of the configurations contributing to the state $|\psi_{k-1,\pi}\rangle$ appears in the expression of the state $\hat{\eta}'_\pi |\psi_k\rangle$ with a unit coefficient (apart from overall normalization factors), then the proof is concluded. Consider any fully-paired Fock state $|c\rangle$ contributing to the state $|\psi_{k-1,\pi}\rangle$. The latter is generated whenever $\hat{\eta}'_\pi$ acts on a configuration contributing to $|\psi_{k,\pi}\rangle$ that can be obtained by adding a pair to the target configuration in $|\psi_{k-1,\pi}\rangle$. The number of such configurations with k pairs equals the expectation value of \hat{C} over the target configuration $|c\rangle$. Therefore, by dividing each contribution that results in $|c\rangle$ by the number of configurations in $|\psi_{k,\pi}\rangle$ that $|c\rangle$ can be reached by, one gets the desired result. This last operation is implemented by the operator expression that precedes the summation over the lattice sites in Eq. (10).

B. Quasi-symmetries

In this Section we draw connections with the quasi-symmetry picture of many-body scar subspaces [66]. Since the spinless η -pairing states $|\psi_{k,\pi}\rangle$ that generate \mathcal{S} are characterized by infinitely long-lived pair quasiparticles, we infer that the total number of pairs \hat{N}_p is a conserved quantity under time evolution within \mathcal{S} . Its explicit form is once more nonlocal, and reads:

$$\hat{N}_p = \sum_{j=1}^{L-1} \hat{P}^{(j-1)} \hat{n}_j \hat{n}_{j+1}. \quad (12)$$

The quasi-symmetry property amounts then to the statement that:

$$\hat{U}_\theta \hat{H} \hat{U}_\theta^\dagger |_{\mathcal{S}} = \hat{H} |_{\mathcal{S}}, \quad (13)$$

where $\hat{U}_\theta = e^{i\theta\hat{N}_p}$ is a unitary representation of $U(1)$. We conclude that the subspace \mathcal{S} enjoys a nontrivial $U(1)$ quasi-symmetry linked to the infinite lifetime of the η -pairs. Similar considerations can be carried out in the case of the operator $\hat{N}_{stag} = \sum_{j=1}^L (-1)^j \hat{n}_j$, which gives rise to an additional $U(1)$ quasisymmetry of the subspace \mathcal{S} via the unitary representation $\hat{U}_\varphi = e^{i\varphi\hat{N}_{stag}}$, which enjoys the properties of being a tensor product representation over the Hilbert spaces attached to the lattice sites.

We underline that, according to the definition of quasi-symmetry of a degenerate subspace [66], the unitary representations are required to be tensor product representations over the Hilbert spaces attached to the lattice sites, in order to avoid including complicated transformations without a transparent physical meaning in the definition. While the latter condition is met by the unitary \hat{U}_φ , it is not satisfied by \hat{U}_θ . However, given the clear physical meaning of the generator \hat{N}_p , we choose to include it in the discussion.

C. Dynamics and quantum coherence

The consequences of Eq. (3) on the dynamics of a generic superposition of the states $|\psi_{k,\pi}\rangle$ are easily computed. For an initial state of the form:

$$|\psi(0)\rangle = \sum_{k=0}^{L/2} m_k |\psi_{k,\pi}\rangle, \quad \sum_k |m_k|^2 = 1, \quad (14)$$

the Loschmidt echo takes the form:

$$\mathcal{L}(t) = |\langle \psi(0) | \psi(t) \rangle|^2 = \left| \sum_k |m_k|^2 e^{i\frac{2\mu k}{\hbar} t} \right|^2, \quad (15)$$

and is periodic with period $T = |\pi\hbar/\mu|$. Coherently with the interpretation of the states $|\psi_{k,\pi}\rangle$ as condensates of pairs, we find here that their time evolution is dictated by the chemical potential μ [74].

The time evolution of the expectation value of an operator is also easily computed. We take $\hat{c}_j \hat{c}_{j+1}$ as an example of operator that has matrix elements between states whose number of pairs differs by one; assuming periodic boundary conditions and odd L for simplicity, the dynamics of its expectation value reads:

$$\begin{aligned} \langle \psi(t) | \hat{c}_j \hat{c}_{j+1} | \psi(t) \rangle &= \\ &= (-1)^{j+1} e^{i\frac{2\mu t}{\hbar}} \sum_{k=0}^{\lfloor L/2 \rfloor - 1} \frac{m_k^* m_{k+1} \binom{L-2-k}{k}}{\sqrt{\frac{L}{L-k} \binom{L-k}{k} \frac{L}{L-k-1} \binom{L-k-1}{k+1}}}, \end{aligned} \quad (16)$$

and exhibits a periodic oscillating behaviour. The complicated coefficients in terms of binomial appearing inside the summation take an easier expression when we consider the thermodynamic limit at fixed density $n = 2k/L$. Noticeably, in agreement with Eq. (7), it is easy to show that:

$$\lim_{L \rightarrow \infty} \langle \psi_{k,\pi} | \hat{c}_j \hat{c}_{j+1} | \psi_{k+1,\pi} \rangle = (-1)^{j+1} \sqrt{\frac{n}{2-n}} (1-n), \quad (17)$$

which allows to conclude that the thermodynamic limit of the pair correlation function, $\lim_{L \rightarrow \infty} P_k(r)$, equals

$$\lim_{L \rightarrow \infty} \langle \psi_{k+1,\pi} | \hat{c}_j^\dagger \hat{c}_{j+1}^\dagger | \psi_{k,\pi} \rangle \langle \psi_{k,\pi} | \hat{c}_{j+r} \hat{c}_{j+r+1} | \psi_{k+1,\pi} \rangle \quad (18)$$

when $r > 3$. Once more, this expression certifies that the states $|\psi_{k,\pi}\rangle$ feature off-diagonal long-range order.

If the states $|\psi_{k,\pi}\rangle$ can be considered as many-body states with macroscopic coherence and fixed number of particles, states of the form (14) can be used to discuss the macroscopic quantum coherence in the more usual grand-canonical ensemble. We can introduce the α states

$$|\alpha\rangle = \mathcal{N}_\alpha e^{\alpha \hat{\eta}_\pi^\dagger} |0\rangle, \quad \alpha \in \mathbb{C} \quad (19)$$

where \mathcal{N}_α is a normalization constant, and by applying the time-evolution operator on $|\alpha\rangle$, one can easily verify that they remain of the same form, and that the parameter α obeys the time-evolution relation:

$$\alpha(t) = e^{i\frac{2\mu}{\hbar} t} \alpha(0). \quad (20)$$

It is tempting to interpret the α states as the coherent states of a quantum harmonic oscillator, but we stress that even if we assume infinite size, the $\hat{\eta}_\pi$ and $\hat{\eta}_\pi^\dagger$ do not satisfy the canonical commutation relation, and for instance $\hat{\eta}_\pi |\alpha\rangle \neq \alpha |\alpha\rangle$. This follows from the considerations presented above on the algebraic properties of the $\hat{\eta}_\pi^\dagger$.

The oscillatory behavior of the coherence parameter α demonstrates transparently that the state $|\alpha\rangle$ returns to itself after a period T and naturally translates into periodic oscillations in the time evolution of suitably chosen local observables, as demonstrated more generally in Eq. (16).

We probe the macroscopic coherence of the state $|\alpha\rangle$ by evaluating the expression in Eq. (16) for the choice $|\psi(t)\rangle = |\alpha(t)\rangle$. The result takes the following form in the limit $L \rightarrow +\infty$ (see Appendix E):

$$\langle \alpha(t) | e^{i\pi j} \hat{c}_{j+1} \hat{c}_j | \alpha(t) \rangle = \frac{2\alpha(t)}{\sqrt{1+4|\alpha|^2} \left(1 + \sqrt{1+4|\alpha|^2}\right)}. \quad (21)$$

While for small values of α the result reproduces the value obtained for the coherent state obtained from a single bosonic mode, the term in the denominator of Eq. (21) corrects the result for larger values of α and arises from the hard-core nature of the pairs that populate the system.

D. Entanglement

In this subsection we compute the scaling of the entanglement entropy of the $|\psi_{k,\pi}\rangle$ for a bipartition of the system into two halves of length $L/2$. We show that they are entanglement outliers, as they display a logarithmic scaling of the half-chain entanglement entropy. To this end, we consider the density matrix $\rho_{k,\pi} = |\psi_{k,\pi}\rangle \langle \psi_{k,\pi}|$ on a system with L sites and we aim to compute the reduced density matrix for the first $\frac{L}{2}$ sites,

i.e., $\rho_{k,\pi}^{(\frac{L}{2})} = \text{Tr}_{[\frac{L}{2}+1, \dots, L]}(\rho_{k,\pi})$. We choose for simplicity the second Renyi entropy, which is defined as follows:

$$S_{\frac{L}{2},k,\pi} = -\log \left\{ \text{Tr} \left[\left(\rho_{k,\pi}^{(\frac{L}{2})} \right)^2 \right] \right\}. \quad (22)$$

$$S_{\frac{L}{2},k,\pi} = -\log \left\{ \sum_{l=\max\{0, \lceil \frac{N-L/2}{} \rceil\}}^{\min\{\frac{N}{2}, \lfloor \frac{L/2}{} \rfloor\}} \left(\frac{\binom{\frac{L}{2}-\frac{N}{2}+l}{\frac{N}{2}-l} \binom{\frac{L}{2}-l}{l}}{\binom{L-\frac{N}{2}}{\frac{N}{2}}} \right)^2 + \sum_{l=\max\{0, \lceil \frac{N-L/2-1}{} \rceil\}}^{\min\{\frac{N}{2}-1, \lfloor \frac{L/2-1}{} \rfloor\}} \left(\frac{\binom{\frac{L}{2}-\frac{N}{2}+l}{\frac{N}{2}-l-1} \binom{\frac{L}{2}-1-l}{l}}{\binom{L-\frac{N}{2}}{\frac{N}{2}}} \right)^2 \right\}. \quad (23)$$

A more readable analytical expression can be found taking the thermodynamic limit $L \rightarrow \infty$ and $k \rightarrow \infty$ and fixing the ratio $2k/L = n = 2/3$. In this limit, in Appendix F we show that the formula is well approximated by:

$$S_{\frac{L}{2},k=\frac{L}{3},\pi} \xrightarrow{L \rightarrow \infty} \frac{1}{2} \log \left(\frac{6\pi L}{25} \right). \quad (24)$$

For more clarity, we have evaluated the resulting entanglement entropy scaling law in Fig. 1(Left), where the analytical prediction in Eq. (23) is plotted as a function of $\log L$ for several choices of the system filling, i.e., of the number of pairs. The figure confirms the agreement with the scaling for $n = 2/3$ in Eq. (24) and demonstrates a scaling as $\log L$ for other filling choices. As already mentioned, a logarithmic scaling of the entanglement entropy signals a non-ETH state, and shows the exceptional character of the $|\psi_{k,\pi}\rangle$.

IV. NUMERICAL ANALYSIS

We proceed by providing numerical benchmarks of the scarred eigenstates discussed in the previous sections by performing exact diagonalization simulations with the QuSpin package [75, 76]. We start by presenting the behaviour of the Loschmidt echo $\mathcal{L}(t)$ when the system is initialized either in the superposition of scarred eigenstates $|\psi_1\rangle = \frac{1}{\sqrt{2}}(|\psi_{1,\pi}\rangle + |\psi_{2,\pi}\rangle)$ or in the generic product states $|\psi_2\rangle = \prod_{j=1}^{L/4} \hat{c}_{2j}^\dagger |0\rangle$. The data presented in Fig. 1(Center) show that, while the superposition of scarred eigenstates shows exact revivals, as predicted exactly via Eq. (15), the coherent dynamics of a generic product state displays a phenomenology that is consistent with the loss of memory of the initial state, as generically expected for a thermalizing isolated many-body quantum system. The data confirm therefore that the revivals associated to the existence of an exact tower of states embedded in the spectrum is atypical and not observed when the dynamics of a generic initial state is monitored.

A further check is provided by plotting the half-chain entanglement entropy of a system described by Hamiltonian (1) on a lattice of size $L = 16$ for $N = 6, 8, 10, 12$. The points highlighted in orange in Fig. 1(Right), which refer to the half-chain entanglement entropy of the scarred eigenstates $\{|\psi_{k,\pi}\rangle\}_{k=3}^6$, point towards the anomalously low entanglement content of the scarred eigenstates with respect to generic excited states

An analytical generic formula for any k can be obtained in terms of binomial coefficients, and reads:

of the model. This finding is consistent with the non-thermal nature of the unveiled quantum many-body scars and confirms their nature of exceptional states embedded in an otherwise ETH-satisfying spectrum.

We conclude this section by demonstrating the nonintegrability of Hamiltonian (1) by means of the study of level-spacing statistics. More specifically, we compute the probability density function of the ratio of consecutive level spacings $r_n = s_n/s_{n-1}$ [77, 78], where $s_n = E_{n+1} - E_n$ is the difference between two consecutive energy levels E_n and E_{n+1} in the spectrum. The comparison between the numerical data and the Wigner-Dyson probability distribution for the GOE ensemble provided in Fig. 2(Left) shows a neat quantitative agreement. Moreover, the average of the level-spacing ratio $\tilde{r}_n = \min(s_n, s_{n-1})/\max(s_n, s_{n-1})$ obtained from the numerical data equals $0.52822\dots$, compatibly with the theoretical value $\langle \tilde{r} \rangle = 0.53590\dots$. We are thus able to conclude that the model is not integrable.

V. EXTENSION TO MULTIMERS

In the following, we generalize our findings on many-body scars with η -pairing to the case of multimers of arbitrary size $M \geq 2$ by constructing a family of Hamiltonians \hat{H}_M , such that states composed of many η -multimers of size M are exact many-body scars of the Hamiltonian \hat{H}_M .

The Hamiltonian is the sum of three terms: $\hat{H}_M = \hat{H}_t + \hat{H}_\mu + \hat{H}_J$ and their explicit forms in open boundary conditions

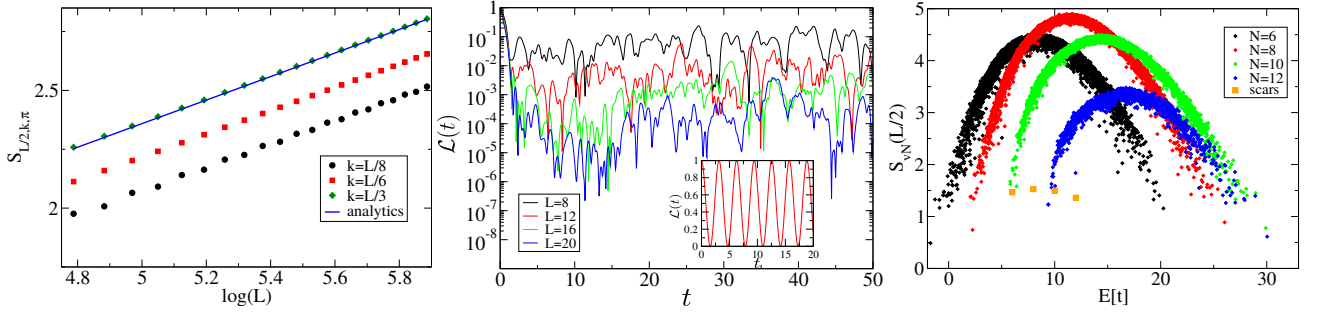


FIG. 1. (Left) Half-chain entanglement entropy of the states $|\psi_{k,\pi}\rangle$ for fillings $n = 2k/L = 1/4, 1/3, 2/3$ according to Eq. (23) as a function of the logarithm of the system size (dots). The blue line is given by the asymptotic expression in Eq. (24). (Center) Loschmidt echo $\mathcal{L}(t)$ of the time-evolved state $|\psi(t)\rangle$ as a function of the elapsed time t for the Hamiltonian parameters $t = 1, J = 2, \mu = -1$, when starting from a product state $|\psi_2\rangle$, see text. Inset: Loschmidt echo $\mathcal{L}(t)$ for a superposition of scarred eigenstates $|\psi_1\rangle$, see text. (Right) Half-chain von Neumann entropy of the eigenstates of Hamiltonian (1) with $t = J = 1, \mu = -1$ on a lattice of size $L = 16$ in the sectors with $N = 6, 8, 10, 12$ particles.

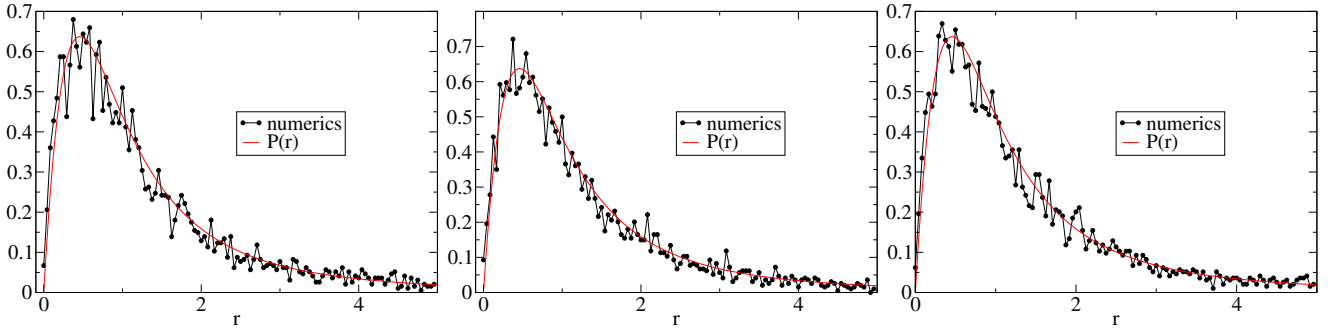


FIG. 2. (Left) The level-spacing statistics of r_n in the middle half of the spectrum of the Hamiltonian in Eq. (1) with OBC with $t = J = 1, \mu = -1$ on a lattice of size $L = 18$ in the inversion symmetry sector $I = -1$ with $N = 6$ particles (black dots) compared to the Wigner-Dyson probability density function for the same quantity (red solid line). (Center) Same plot for the Hamiltonian \hat{H}_3 in Eq. (28) with $t = J = 1, \mu = -1$ on a lattice of size $L = 18$ in the inversion symmetry sector $I = -1$ with $N = 6$ particles. (Right) Same plot for \hat{H}_3 in Eq. (28) with $t = 1, J = 0, \mu = -1$; all other parameters as in the central plot.

read:

$$\hat{H}_t = -t \sum_{j=1}^{L-1} \left[\hat{c}_j^\dagger \hat{c}_{j+1} + H.c. \right] - t \sum_{j=1}^{L-M+1} \left[\hat{M}_{j+1}^\dagger \hat{M}_j + H.c. \right]; \quad (25a)$$

$$\hat{H}_\mu = -\mu \sum_{j=1}^L \hat{n}_j; \quad (25b)$$

$$\hat{H}_J = J \sum_{j=1}^{L-M} \left(\prod_{l=0}^{M-1} \hat{n}_{j+l} + \prod_{l=1}^M \hat{n}_{j+l} - 2 \prod_{l=0}^M \hat{n}_{j+l} + \left[\hat{M}_j^\dagger \hat{M}_{j+1} + H.c. \right] \right). \quad (25c)$$

In the Hamiltonian \hat{H}_t we recognize a single-particle and a $M - 1$ -particle hopping term, with

$$\hat{M}_j^\dagger = \prod_{l=0}^{M-2} \hat{c}_{j+l}^\dagger = \hat{c}_j^\dagger \dots \hat{c}_{j+M-2}^\dagger, \quad (26)$$

whereas \hat{H}_μ is just a chemical potential term. The Hamil-

tonian \hat{H}_J is a frustration-free positive Hamiltonian of the form $J \sum_j \hat{L}_j^{\dagger(M)} \hat{L}_j^{(M)}$, comprising both density-density interactions and a M -particle hopping term:

$$\hat{M}_j^\dagger = \prod_{l=0}^{M-1} \hat{c}_{j+l}^\dagger = \hat{c}_j^\dagger \dots \hat{c}_{j+M-1}^\dagger. \quad (27)$$

The explicit expression of $\hat{L}_j^{(M)}$, that is inessential for this discussion, is given in Appendix G. For completeness, we mention that multimer Hamiltonians and variants thereof have been discussed in Refs. [73, 79].

The Hamiltonian \hat{H}_M is the generalisation of the Hamiltonian \hat{H} introduced in Eq. (1) and it reduces exactly to it for $M = 2$. A particularly interesting property is the fact that for $M \geq 3$ the simpler Hamiltonian $\hat{H}_t + \hat{H}_\mu$ is already not integrable; for $M = 2$ this would not be true as it would be a free-fermion model. We verify this first statement with a numerical analysis for the case $M = 3$, and for reading convenience we write here the explicit Hamiltonian:

$$\hat{H}_3 = -t \sum_{j=1}^{L-1} (\hat{c}_j^\dagger \hat{c}_{j+1} + H.c.) - \mu \sum_{j=1}^L \hat{n}_j + t \sum_{j=1}^{L-2} (\hat{c}_{j+2}^\dagger \hat{n}_{j+1} \hat{c}_j + H.c.) + J \sum_{j=1}^{L-3} [\hat{n}_j \hat{n}_{j+1} \hat{n}_{j+2} + \hat{n}_{j+1} \hat{n}_{j+2} \hat{n}_{j+3} - 2\hat{n}_j \hat{n}_{j+1} \hat{n}_{j+2} \hat{n}_{j+3} + (\hat{c}_j^\dagger \hat{n}_{j+1} \hat{n}_{j+2} \hat{c}_{j+3} + H.c.)]. \quad (28)$$

First of all, we study its level-spacing statistics, as in the case of η -pairs. The results shown in Fig. 2(center) and (right) showcase the agreement between the Wigner-Dyson distribution and the numerical data. For $J \neq 0$, the value of $\langle \tilde{r} \rangle$ is computed from the numerics to be $0.5296 \dots$, which is compatible with its theoretical prediction. For $J = 0$, the average of $\langle \tilde{r} \rangle$ computed numerically takes the value $0.5326 \dots$. We conclude that the deformation of the Hamiltonian proportional to J is not necessary to make the model nonintegrable when working with $M = 3$ and we expect this to be true in general for $M > 2$.

We assume open boundary conditions and introduce the corresponding tower of states $|\psi_{k,\pi}^{(M)}\rangle$ that generalise those presented in Eq. (2); for M even they are condensates of multimers at $k = \pi$:

$$|\psi_{k,\pi}^{(M)}\rangle = \frac{(\hat{\eta}_\pi^\dagger)^k}{k! \sqrt{\binom{L-(M-1)k}{k}}} |0\rangle, \quad \hat{\eta}_\pi^\dagger = \sum_j e^{i\pi j} \hat{M}_j^\dagger. \quad (29)$$

For M odd, the multimers are fermionic, and the notion of condensation cannot be applied. In this case the scar states are the equal-amplitude superposition of all multimer states weighted by a phase factor. To make this precise, we need to define what a multimer state, namely a real-space Fock state of the spinless fermions where fermions bunch in groups whose length is a multiple of M . For $M = 3$, for instance, $|\bullet\bullet\bullet\circ\circ\circ\circ\rangle$ and $|\circ\bullet\bullet\bullet\bullet\circ\circ\rangle$ are multimer states, whereas $|\bullet\bullet\bullet\circ\circ\circ\rangle$ is not. To each multimer state we can associate the phase factor $e^{i\pi \sum_j m_j}$, where m_j is the site where the first fermion of the j -th multimer is located. For the two multimer states given above, in the first case $m_1 = 2$, and in the second case $m_1 = 2$ and $m_2 = 5$. The linear superposition of all multimer states multiplied by the given phase factors defines the exact scars; it is not difficult to observe that these states generalise the properties of the bosonic states defined above.

In order to verify the peculiar properties of multimer scars, we focus on the specific case $M = 3$ and we probe the existence of such towers of states with numerical tools: we will show the existence of atypical eigenstates with energies $E_k = -M\mu k$, $k = 0, \dots, \lfloor L/M \rfloor$. It is interesting to observe that in the fermionic case the tower of states are not generated by a local raising operator, as it happens in the bosonic case.

We test the half-chain von Neumann entanglement entropy in Fig. 3, where the atypical eigenstates belonging to the tower of states defined in Eq. (25a) with $M = 3$ emerge as entangle-

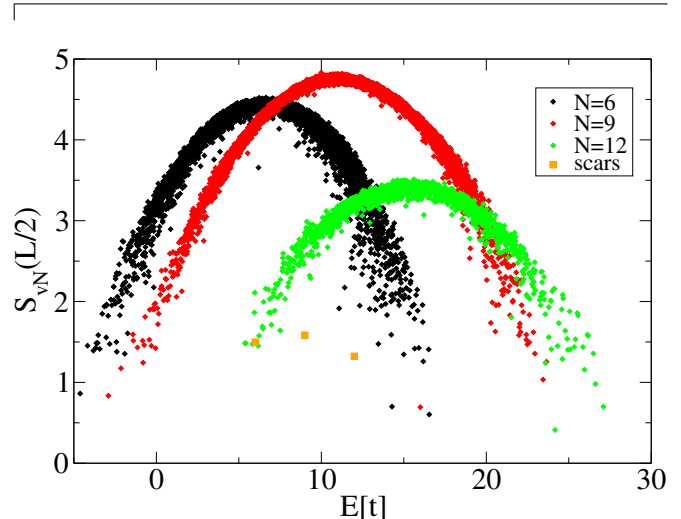


FIG. 3. Half-chain von Neumann entanglement entropy of the eigenstates of the Hamiltonian \hat{H}_3 with $t = J = 1$, $\mu = -1$ on a lattice of size $L = 16$ in the sectors with $N = 6, 9, 12$ particles.

ment outliers with respect to the typical behavior observed for generic highly-excited eigenstates. We also show in Fig. 4 the expectation value of a generic local observable related to the relevant quasiparticles, in this case the total trimer-hopping energy density

$$K_3 = \frac{1}{L} \sum_{j=1}^{L-3} \langle \hat{c}_j^\dagger \hat{n}_{j+1} \hat{n}_{j+2} \hat{c}_{j+3} + H.c. \rangle. \quad (30)$$

The plot shows that K_3 takes an anomalous value when evaluated over the scarred eigenstate $|\psi_{3,\pi}^{(3)}\rangle$, whereas it behaves as smooth function of energy for the other eigenstates, thereby supporting the validity of the weak ETH-breaking associated to the scars that we are presenting.

VI. CONCLUSIONS

In this article, we have studied several models of spinless fermions with exact many-body scars that are based on pairs or multimer bound states. In the first part, we have focused on the case of condensates of pairs. We have characterized exactly the spectral and entanglement properties of the tower of eigenstates responsible for their emergence, thereby proving that the latter display subvolume entanglement entropy scaling and that they are energetically equally-spaced. The afore-

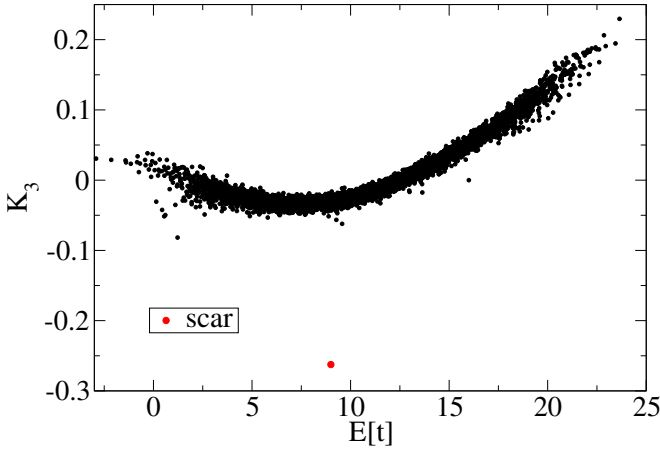


FIG. 4. Expectation value K_3 over the eigenstates of Hamiltonian \hat{H}_3 for $t = J = 1$, $\mu = -1$ on a lattice of size $L = 16$ for $N = 9$ particles.

mentioned results are corroborated by the numerical analysis of the Loschmidt echo and of the half-chain entanglement entropy, which give clear evidence of the exceptional character of the dynamical properties exhibited by the scarred eigenstates. The latter are indeed atypical, as generic excited eigenstates of the model Hamiltonian are expected to possess standard thermalization properties described within the framework of ETH. Finally, the level-spacing statistics reveals that the system is not integrable and hence that the ETH-breaking involves only a measure-zero set of eigenstates of the Hamiltonian. The results are then generalised in the second part of the article, where we focus on multimers. The Hamiltonian that we propose is simpler than in the pair case, whereas the scars generalise in many aspects the properties of the pair condensates. We have highlighted the fact that for fermionic multimers there cannot be condensation and we could not find local raising or lowering operators generating the tower of states.

The unveiled results open the route towards further investigations. On one side, it will be interesting to investigate whether such a construction is amenable to generalizations to two-dimensional and, more generically, higher-dimensional setups. The spatial structure of the pair and multimer complicates the algebraic relations and makes such an extension non-trivial. On the other side, a stimulating challenge for the future would consist in devising quantum-state engineering protocols to prepare the system in the discovered scar states or in a state that is sufficiently close to it to make the revivals visible in an experiment with a quantum simulator.

Note: recently, an article by K. Tamura and H. Katsura has presented results overlapping with ours [80]. Our results have been derived independently. We also acknowledge the observation by H. Katsura that a Jordan-Wigner transformation maps the pairing Hamiltonian in Eq. (1) to a specific instance of the model discussed in Ref. [43].

ACKNOWLEDGMENTS

We acknowledge funding by LabEx PALM (ANR-10-LABX-0039-PALM). This work has been supported by Region Ile-de-France in the framework of the DIM Sirteq.

Appendix A: Proof of Eq. (3)

1. Proof by direct verification

In order to assert the validity of Eq. (3), we consider the Hamiltonian $\hat{H}_0 = \hat{U}_0 \hat{H} \hat{U}_0^\dagger$ and prove the analogous relation:

$$\hat{H}_0 |\psi_{k,0}\rangle = -2\mu k |\psi_{k,0}\rangle. \quad (\text{A1})$$

Combining Eq. (A1) and Eq. (F3) with the definition of \hat{H}_0 , we obtain the desired result presented in Eq. (3).

To this end, let us consider more explicitly the expression of \hat{H}_0 :

$$\begin{aligned} \hat{H}_0 = & it \sum_{j=1}^{L-1} [\hat{c}_j^\dagger \hat{c}_{j+1} - c_{j+1}^\dagger \hat{c}_j] - \mu \sum_{j=1}^L \hat{n}_j + \\ & + 2J \sum_{j=1}^{L-2} [\hat{n}_j \hat{n}_{j+1} + \hat{n}_{j+1} \hat{n}_{j+2} - 2\hat{n}_j \hat{n}_{j+1} \hat{n}_{j+2} + \\ & + (\hat{c}_j^\dagger \hat{n}_{j+1} \hat{c}_{j+2} + H.c.)]. \end{aligned} \quad (\text{A2})$$

The action of the single-particle hopping term in Eq. (A2) on the states $|\psi_{k,0}\rangle$ can be evaluated as follows:

$$\begin{aligned} it \sum_{j=1}^{L-1} [\hat{c}_j^\dagger \hat{c}_{j+1} - c_{j+1}^\dagger \hat{c}_j] |\psi_{k,0}\rangle = & \quad (\text{A3}) \\ = it \left[\sum_{j=1}^{L-2} \hat{c}_j^\dagger \hat{c}_{j+1} - \sum_{j=2}^{L-1} \hat{c}_{j+1}^\dagger \hat{c}_j \right] |\psi_{k,0}\rangle = \\ = it \sum_{j=1}^{L-2} [(\hat{c}_j^\dagger - \hat{c}_{j+2}^\dagger) \hat{c}_{j+1}] |\psi_{k,0}\rangle, \end{aligned}$$

where we have discarded the terms $\hat{c}_2^\dagger \hat{c}_1$ and $\hat{c}_{L-1}^\dagger \hat{c}_L$ when going from the first to the second row since their action vanishes on fully paired Fock basis configurations. After the above manipulations, and denoting as \mathcal{C} the set of all pair configurations contributing to the equal-weight superposition defining the state $|\psi_{k,0}\rangle$, let us evaluate:

$$\begin{aligned} (\hat{c}_j^\dagger - \hat{c}_{j+2}^\dagger) \hat{c}_{j+1} |\psi_{k,0}\rangle = & \quad (\text{A4}) \\ = \frac{1}{k! \sqrt{\binom{L-k}{k}}} \left[\sum_{\substack{c \in \mathcal{C}: \\ \langle \hat{n}_j \rangle = 0, \\ \langle \hat{n}_{j+1} \rangle = 1, \\ \langle \hat{n}_{j+2} \rangle = 1}} |\dots \circ \circ \dots\rangle - \sum_{\substack{c \in \mathcal{C}: \\ \langle \hat{n}_j \rangle = 1, \\ \langle \hat{n}_{j+1} \rangle = 1, \\ \langle \hat{n}_{j+2} \rangle = 0}} |\dots \circ \circ \dots\rangle \right] \\ = 0. \end{aligned}$$

As the above relation holds for $j = 1, \dots, L-2$, one obtains:

$$it \sum_{j=1}^{L-1} \left[\hat{c}_j^\dagger \hat{c}_{j+1} - c_{j+1}^\dagger \hat{c}_j \right] |\psi_{k,0}\rangle = 0. \quad (\text{A5})$$

The action of the chemical potential on the states $|\psi_{k,\pi}\rangle$ is trivial, as it amounts to counting the number of particles in the given state, and reads:

$$-\mu \sum_{j=1}^L \hat{n}_j |\psi_{k,0}\rangle = -2\mu k |\psi_{k,0}\rangle. \quad (\text{A6})$$

Finally, in order to evaluate the action of the interacting term on $|\psi_{k,0}\rangle$, it is convenient to rewrite it as:

$$2J \sum_{j=1}^{L-2} [\hat{n}_j \hat{n}_{j+1} + \hat{n}_{j+1} \hat{n}_{j+2} - 2\hat{n}_j \hat{n}_{j+1} \hat{n}_{j+2} + \quad (\text{A7})$$

$$+ (\hat{c}_j^\dagger \hat{n}_{j+1} \hat{c}_{j+2} + H.c.)] = 2J \sum_{j=1}^{L-2} \hat{U}_0 \hat{L}_j^\dagger \hat{U}_0^\dagger \hat{U}_0 \hat{L}_j \hat{U}_0^\dagger, \quad (\text{A8})$$

where:

$$\hat{U}_0 \hat{L}_j \hat{U}_0^\dagger = \hat{n}_j \hat{n}_{j+1} - \hat{n}_{j+1} \hat{n}_{j+2} - \hat{c}_{j+2}^\dagger \hat{n}_{j+1} \hat{c}_j + \hat{c}_j^\dagger \hat{n}_{j+1} \hat{c}_{j+2}. \quad (\text{A9})$$

Hence, it suffices to prove that $\hat{U}_0 \hat{L}_j \hat{U}_0^\dagger |\psi_{k,0}\rangle = 0$. By denoting as \mathcal{C} the set of all pair configurations contributing to the equal-weight superposition defining the state $|\psi_{k,0}\rangle$, we obtain:

$$\begin{aligned} \hat{U}_0 \hat{L}_j \hat{U}_0^\dagger |\psi_{k,0}\rangle &= \frac{1}{k! \sqrt{\binom{L-k}{k}}} \left[\sum_{\substack{c \in \mathcal{C}: \\ \langle \hat{n}_j \rangle = 1, \\ \langle \hat{n}_{j+1} \rangle = 1}} |c\rangle - \sum_{\substack{c \in \mathcal{C}: \\ \langle \hat{n}_{j+1} \rangle = 1, \\ \langle \hat{n}_{j+2} \rangle = 1}} |c\rangle + \right. \\ &\quad \left. + \sum_{\substack{c \in \mathcal{C}: \\ \langle \hat{n}_j \rangle = 0, \\ \langle \hat{n}_{j+1} \rangle = 1, \\ \langle \hat{n}_{j+2} \rangle = 1}} |c\rangle - \sum_{\substack{c \in \mathcal{C}: \\ \langle \hat{n}_j \rangle = 1, \\ \langle \hat{n}_{j+1} \rangle = 1, \\ \langle \hat{n}_{j+2} \rangle = 0}} |c\rangle \right] = 0, \end{aligned} \quad (\text{A10})$$

where the final result is obtained by combining the first and last summation and the second and third summation, respectively. The result presented in Eq. (3) is thus proved.

2. Algebraic proof

We follow yet another, more rigorous route to prove Eq. (3). We aim at showing that, for $k = 0, \dots, \lfloor \frac{L}{2} \rfloor$, the following is

true:

$$\left(-t \sum_{j=1}^{L-1} [\hat{c}_j^\dagger \hat{c}_{j+1} + H.c.] + J \sum_{j=1}^{L-2} \hat{L}_j^\dagger \hat{L}_j \right) |\psi_{k,\pi}\rangle = 0. \quad (\text{A11})$$

We start by considering the single-particle hopping term. In this case, it is straightforward to show that:

$$\left[-t \sum_{j=1}^{L-1} \left(\hat{c}_j^\dagger \hat{c}_{j+1} + H.c. \right), \hat{n}_\pi^\dagger \right] = -\hat{c}_1^\dagger \hat{c}_3^\dagger + \quad (\text{A12})$$

$$+ \sum_{j=2}^{L-2} (-1)^j \left(\hat{c}_{j-1}^\dagger \hat{c}_{j+1}^\dagger + \hat{c}_j^\dagger \hat{c}_{j+2}^\dagger \right) + (-1)^{L-1} \hat{c}_{L-2}^\dagger \hat{c}_L^\dagger = 0, \quad (\text{A13})$$

which trivially implies:

$$-t \sum_{j=1}^{L-1} \left(\hat{c}_j^\dagger \hat{c}_{j+1} + H.c. \right) |\psi_{k,\pi}\rangle = 0, \quad k = 0, \dots, \lfloor \frac{L}{2} \rfloor \quad (\text{A14})$$

On the other hand, if we denote $\hat{H}_{int} = J \sum_{j=1}^{L-2} \hat{L}_j^\dagger \hat{L}_j$, in order to prove $\hat{H}_{int} |\psi_{k,\pi}\rangle = 0$, we need a preparatory lemma.

Lemma 1. *Let us consider a Hamiltonian \hat{H} and a set of nonzero states $\{(\hat{A}^\dagger)^k |0\rangle\}_{k=0}^N$ obtained by repeated application of the operator \hat{A}^\dagger to the vacuum. Let us further define:*

$$\hat{H}_0 = \hat{H}, \quad (\text{A15})$$

$$\hat{H}_1 = [\hat{H}, \hat{A}^\dagger], \quad (\text{A16})$$

$$\hat{H}_k = [\hat{H}_{k-1}, \hat{A}^\dagger], \quad 2 \leq k \leq N. \quad (\text{A17})$$

Then, if $\hat{H}_k |0\rangle = 0$ for $k = 0, \dots, N$, one has:

$$\hat{H} \left(\hat{A}^\dagger \right)^k |0\rangle = 0, \quad k = 0, \dots, N \quad (\text{A18})$$

Proof.

We prove the lemma by showing by induction that:

$$\hat{H} (\hat{A}^\dagger)^n = \sum_{k=0}^n \binom{n}{k} (\hat{A}^\dagger)^k \hat{H}_{n-k}, \quad k = 0, \dots, N. \quad (\text{A19})$$

The base case $k = 0$ is trivially verified. Thus, let us assume the result is proven for $0 \leq k \leq n$ and show that it holds as a result for $k = n+1$ as well. We perform the following manipulations:

$$\begin{aligned}\hat{H}(\hat{A}^\dagger)^{n+1} &= \left[\sum_{k=0}^n \binom{n}{k} (\hat{A}^\dagger)^k \hat{H}_{n-k} \right] \hat{A}^\dagger = \sum_{k=0}^n \binom{n}{k} (\hat{A}^\dagger)^k \left[\hat{H}_{n+1-k} + \hat{A}^\dagger \hat{H}_{n-k} \right] = \\ &= \hat{H}_{n+1} + \sum_{k=1}^n \left[\binom{n}{k} + \binom{n}{k-1} \right] (\hat{A}^\dagger)^k \hat{H}_{n+1-k} + (\hat{A}^\dagger)^{n+1} \hat{H}_0 = \sum_{k=0}^{n+1} \binom{n+1}{k} (\hat{A}^\dagger)^k \hat{H}_{n+1-k},\end{aligned}\quad (\text{A20})$$

thus proving the result. The lemma follows trivially from the assumption that $\hat{H}_k |0\rangle = 0$ for $k = 0, \dots, N$.

We wish to apply the above lemma to the hamiltonian \hat{H}_{int} and the set of states $\{(\hat{\eta}_\pi^\dagger)^k |0\rangle\}_{k=0}^{\lfloor \frac{L}{2} \rfloor}$. To this end, let us consider the parameter-dependent state:

$$|\psi(\alpha)\rangle = e^{\alpha \hat{\eta}_\pi^\dagger} \hat{H}_{int} e^{-\alpha \hat{\eta}_\pi^\dagger} |0\rangle. \quad (\text{A21})$$

On one hand, it can be shown that $|\psi(\alpha)\rangle = 0$ by rewriting $|\psi(\alpha)\rangle$ as:

$$\begin{aligned}|\psi(\alpha)\rangle &= e^{\alpha \hat{\eta}_\pi^\dagger} \left(\sum_{j=1}^{L-2} \hat{L}_j^\dagger \hat{L}_j \right) e^{-\alpha \hat{\eta}_\pi^\dagger} |0\rangle = \prod_{j=1}^3 e^{\alpha(-1)^j \hat{c}_j^\dagger \hat{c}_{j+1}^\dagger} \hat{L}_1^\dagger \hat{L}_1 \prod_{j=1}^3 e^{-\alpha(-1)^j \hat{c}_j^\dagger \hat{c}_{j+1}^\dagger} |0\rangle + \\ &+ \sum_{j=2}^{L-3} \prod_{k=j-1}^{j+2} e^{\alpha(-1)^k \hat{c}_k^\dagger \hat{c}_{k+1}^\dagger} \hat{L}_j^\dagger \hat{L}_j \prod_{k=j-1}^{j+2} e^{-\alpha(-1)^k \hat{c}_k^\dagger \hat{c}_{k+1}^\dagger} |0\rangle + \prod_{j=L-3}^{L-1} e^{\alpha(-1)^j \hat{c}_j^\dagger \hat{c}_{j+1}^\dagger} \hat{L}_{L-2}^\dagger \hat{L}_{L-2} \prod_{j=L-3}^{L-1} e^{-\alpha(-1)^j \hat{c}_j^\dagger \hat{c}_{j+1}^\dagger} |0\rangle\end{aligned}\quad (\text{A22})$$

and showing that each term in the above summation vanishes.

On the other hand, the Baker-Campbell-Hausdorff formula allows to express the latter as:

$$|\psi(\alpha)\rangle = \hat{H}_{int} |0\rangle + \alpha [\hat{\eta}_\pi^\dagger, \hat{H}_{int}] |0\rangle + \frac{\alpha^2}{2!} [\hat{\eta}_\pi^\dagger, [\hat{\eta}_\pi^\dagger, \hat{H}_{int}]] |0\rangle + \dots, \quad (\text{A23})$$

up to order $\lfloor \frac{L}{2} \rfloor$. As $|\psi(\alpha)\rangle$ vanishes, each of the states multiplying the corresponding power of α must vanish. Hence, the conditions of the lemma are satisfied and Eq. (A11) is proved, which in turn implies the validity of Eq. (3).

Appendix B: Coordinate Bethe Ansatz in the fully paired subspace for the interacting term in Hamiltonian (1)

We start from the spinless fermion Hamiltonian (1) with $t = \mu = 0$ and rewrite it in PBC with a change in the sign of the pair hopping for the terms across the bond among sites L and 1:

$$\hat{H} = J \sum_{j=1}^{L-2} \left[\hat{n}_j \hat{n}_{j+1} + \hat{n}_{j+1} \hat{n}_{j+2} - 2\hat{n}_j \hat{n}_{j+1} \hat{n}_{j+2} - (\hat{c}_j^\dagger \hat{n}_{j+1} \hat{c}_{j+2} + H.c.) \right] + \quad (\text{B1})$$

$$+ J \left[\hat{n}_{L-1} \hat{n}_L + \hat{n}_L \hat{n}_1 - 2\hat{n}_{L-1} \hat{n}_L \hat{n}_1 + (\hat{c}_{L-1}^\dagger \hat{n}_L \hat{c}_1 + H.c.) \right] + \quad (\text{B2})$$

$$+ J \left[\hat{n}_L \hat{n}_1 + \hat{n}_1 \hat{n}_2 - 2\hat{n}_L \hat{n}_1 \hat{n}_2 + (\hat{c}_L^\dagger \hat{n}_1 \hat{c}_2 + H.c.) \right]. \quad (\text{B3})$$

When rewritten in spin-1/2 language and in the sector of even parity (that the fully paired subspace belongs to), it takes the form:

$$\hat{H} = J \sum_{j=1}^L \left[\hat{n}_j \hat{n}_{j+1} + \hat{n}_{j+1} \hat{n}_{j+2} - 2\hat{n}_j \hat{n}_{j+1} \hat{n}_{j+2} + (\hat{\sigma}_j^+ \hat{n}_{j+1} \hat{\sigma}_{j+2}^- + H.c.) \right], \quad (\text{B4})$$

where $\hat{n}_j = \frac{1+\hat{\sigma}_j^z}{2}$. In the following, we apply the coordinate Bethe Ansatz technique to the subspace spanned by fully

paired configurations and write down Bethe equations for the momenta of the pairs first in the 1-pair problem and then in the

2-pair one, showing the lack of interactions among η -pairs.

1. 1-pair problem

We search for a generic eigenstate in the 1-pair subspace by writing it in the form:

$$|\psi\rangle = \sum_{j=1}^L a(j) \hat{\sigma}_j^+ \hat{\sigma}_{j+1}^+ |\downarrow\rangle, \quad (\text{B5})$$

where $|\downarrow\rangle$ is the spin down ferromagnetic state. The Schroedinger equation $\hat{H}|\psi\rangle = E|\psi\rangle$ and the periodic boundary conditions read:

$$2Ja(j) + Ja(j-1) + Ja(j+1) = Ea(j), \quad (\text{B6})$$

$$a(L+j) = a(j). \quad (\text{B7})$$

Looking for a solution of the form $a(j) = Ae^{ikj}$, one obtains the conditions:

$$E = 2J + 2J \cos(k) \quad (\text{B8})$$

$$k = \frac{2\pi}{L}n, \quad n = 0, \dots, L-1. \quad (\text{B9})$$

When L is even, the 1-pair eta-pairing state $|\psi\rangle \propto \left(\sum_{j=1}^L e^{i\pi j} \hat{\sigma}_j^+ \hat{\sigma}_{j+1}^+\right) |\downarrow\rangle$ is recovered.

2. 2-pair problem

We search for a generic eigenstate in the 2-pair subspace by writing it in the form:

$$|\psi\rangle = \sum_{1 \leq j_1 < j_2 \leq L} a(j_1, j_2) \hat{\sigma}_{j_1}^+ \hat{\sigma}_{j_1+1}^+ \hat{\sigma}_{j_2}^+ \hat{\sigma}_{j_2+1}^+ |\downarrow\rangle, \quad (\text{B10})$$

where one should notice that the term multiplying $a(j_1, j_1+1)$ vanishes. The Schroedinger equation $\hat{H}|\psi\rangle = E|\psi\rangle$ reads now:

$$4Ja(j_1, j_2) + Ja(j_1-1, j_2) + Ja(j_1+1, j_2) + Ja(j_1, j_2-1) + Ja(j_1, j_2+1) = Ea(j_1, j_2), \quad j_2 > j_1+2 \quad (\text{B11})$$

$$2Ja(j_1, j_1+2) + Ja(j_1-1, j_2) + Ja(j_1, j_1+3) = Ea(j_1, j_1+2), \quad j_2 = j_1+2, \quad (\text{B12})$$

while PBC are enforced through the equation:

$$a(j_1, j_2) = a(j_2, j_1+L). \quad (\text{B13})$$

The Ansatz for the coefficients $a(j_1, j_2)$ takes the form:

$$a(j_1, j_2) = A_{12}e^{i(k_1j_1+k_2j_2)} + A_{21}e^{i(k_2j_1+k_1j_2)}. \quad (\text{B14})$$

The above Ansatz solves Eq. (B11) with energy $E = 4J + 2J \cos(k_1) + 2J \cos(k_2)$, while Eq. (B12) is solved by adding to it the terms such that it takes the same form as Eq. (B11) and setting them to zero. The result of this procedure leads to the condition:

$$2Ja(j_1, j_1+2) + Ja(j_1+1, j_1+2) + Ja(j_1, j_1+1) = 0, \quad (\text{B15})$$

that amounts to requiring that:

$$\frac{A_{21}}{A_{12}} = -\frac{2e^{i2k_2} + e^{i(k_1+2k_2)} + e^{ik_2}}{2e^{i2k_1} + e^{i(k_2+2k_1)} + e^{ik_1}} := S(k_1, k_2), \quad (\text{B16})$$

where we have defined the scattering matrix $S(k_1, k_2)$ via the expression to its left.

Finally, imposing PBC, one obtains the relations:

$$A_{12} = A_{21}e^{ik_1L}, \quad (\text{B17})$$

$$A_{21} = A_{12}e^{ik_2L}, \quad (\text{B18})$$

which, owing to the property $S(k, k) = -1$, can be rewritten in the compact form:

$$\prod_{l=1}^2 S(k_j, k_l) = -e^{-ik_jL}; \quad j = 1, 2. \quad (\text{B19})$$

The result can be shown to generalize to the nontrivial three-pair case, thus proving the Bethe- Ansatz solvability of model (B4) in the subspace spanned by fully-paired configurations.

It should be noticed that the two-pair η -pairing state, obtained for $k_1 = k_2 = \pi$, satisfies Eq. (B15) for all values of A_{12}, A_{21} and the PBC in Eq. (B13) for an even value of L , which impose $A_{12} = A_{21}$. The scattering matrix is ill-defined in this case, as the coefficient $a(j_1, j_2)$ reduces to:

$$a(j_1, j_2) \propto e^{i\pi j_1} e^{i\pi j_2}, \quad (\text{B20})$$

i.e., it factorizes into independent plane waves with quasimomentum π .

Appendix C: Finite-size formula for $P_k(r)$

We present here an explicit finite-size formula for $P_k(r)$ with $r > 3$. Straightforward combinatorial considerations give the result:

$$P_k(r) = (-1)^{r+1} \frac{\sum_{l=\max(0, k-1-\lfloor \frac{r-2}{2} \rfloor)}^{\min(k-1, \lfloor \frac{r-2}{2} \rfloor)} \binom{r-2-l}{l} \binom{L-1-r-k+l}{k-l-1} j_m}{\frac{L}{L-k} \binom{L-k}{k}} \quad (C1)$$

Appendix D: The operator \hat{O} annihilates the tower of states

The operator \hat{O} takes the form $\hat{O} = J \sum_{j=2}^{L-2} \hat{O}_j$, where:

$$\begin{aligned} \hat{O}_j = & e^{i\pi(j-1)} (1 - 2\hat{n}_{j-1}) \hat{n}_j \hat{c}_{j+1}^\dagger \hat{c}_{j+2}^\dagger + \\ & + e^{i\pi(j-1)} \hat{c}_{j-1}^\dagger \hat{c}_j^\dagger \hat{n}_{j+1} (1 - 2\hat{n}_{j+2}) + \\ & + e^{i\pi j} \hat{c}_{j-1}^\dagger (\hat{n}_j + \hat{n}_{j+1}) \hat{c}_{j+2}^\dagger. \end{aligned} \quad (D1)$$

$$\hat{O}_j |\psi_{k,\pi}\rangle = e^{i\pi j} \left(\sum_{c:|\bullet\bullet\bullet\circ\rangle} e^{i\pi \text{sgn}(c)} |\bullet\bullet\bullet\bullet\rangle + \sum_{c:|\circ\bullet\bullet\bullet\rangle} e^{i\pi \text{sgn}(c)} |\bullet\bullet\bullet\bullet\rangle + 2 \sum_{c:|\circ\bullet\bullet\circ\rangle} e^{i\pi \text{sgn}(c)} |\bullet\bullet\bullet\bullet\rangle \right). \quad (D2)$$

The number of configurations contributing to the state $|\psi_{k,\pi}\rangle$ that locally, on sites $j-1, j, j+1, j+2$, have the form $|\bullet\bullet\bullet\circ\rangle$ is equal to the number of those with the forms $|\circ\bullet\bullet\bullet\rangle$ and $|\circ\bullet\bullet\circ\rangle$, and they can be put in a one-to-one correspondence with each other by mapping each configuration in of the afore-said three collections to the one that is identical to it up to the different occupation of the highlighted sites $j-1, j, j+1, j+2$. Since the local configuration resulting from the application of \hat{O}_j is the same in all three cases, the three summations are carried over the same set of configurations. On the other hand, the sign of each of the configurations in the last summation is the opposite of the sign of the corresponding ones in the first two summations, leading to the desired result $\hat{O}_j |\psi_{k,\pi}\rangle = 0$.

Appendix E: Macroscopic coherence of the state $|\alpha\rangle$

We derive here explicitly the result shown in Eq. (21). The explicit expression for the state $|\alpha\rangle$ reads:

$$|\alpha\rangle = \mathcal{N} \sum_{k=0}^{L/2} \sqrt{\frac{L}{L-k} \binom{L-k}{k}} \alpha^k |\psi_{k,\pi}\rangle, \quad (E1)$$

Hence, it suffices to show that $\hat{O}_j |\psi_{k,\pi}\rangle = 0$ for $2 \leq j \leq L-2$. We adopt the notation $\sum_{c:|x_1,\dots,x_4\rangle} e^{i\pi \text{sgn}(c)} |y_1, \dots, y_4\rangle$ to denote the sum over all Fock states $|c\rangle$ contributing to the state $|\psi_{k,\pi}\rangle$ that have the form $|x_1, \dots, x_4\rangle$ on sites $j-1, j, j+1, j+2$ prior to the application of \hat{O}_j and the form $|y_1, \dots, y_4\rangle$ after the application of \hat{O}_j , and where $\text{sgn}(c) = \sum_{m=1}^k j_m$, j_m being the position of the first fermion of the m^{th} pair in the state $|\psi_{k,\pi}\rangle$. Then, it is easy to obtain:

where the normalization constant \mathcal{N} satisfies:

$$|\mathcal{N}|^2 = \frac{1}{\sum_{k=0}^{L/2} \frac{L}{L-k} \binom{L-k}{k} |\alpha|^{2k}} \quad (E2)$$

which results from imposing the normalization condition $\langle \alpha | \alpha \rangle = 1$.

Plugging the expression of the expansion coefficients in Eq. (E1) into Eq. (16), one obtains:

$$\langle \alpha(t) | e^{i\pi j} \hat{c}_{j+1} \hat{c}_j | \alpha(t) \rangle = \alpha e^{i\frac{2\pi t}{k}} \frac{\sum_{k=0}^{L/2-1} \binom{L-k-2}{k} |\alpha|^{2k}}{\sum_{k=0}^{L/2} \frac{L}{L-k} \binom{L-k}{k} |\alpha|^{2k}}. \quad (E3)$$

If we assume self-consistently that the sums in the numerator and denominator of Eq. (E3) will be dominated by terms with $k = O(L)$ and apply Stirling's approximation $n! \approx \sqrt{2\pi n} n^n e^{-n}$, one obtains, as a function of the rescaled variable $x = \frac{3k}{L}$:

$$\frac{L}{L-k} \binom{L-k}{k} |\alpha|^{2k} \approx g(x) e^{\frac{L}{3} f(x)}, \quad (E4)$$

$$\binom{L-k-2}{k} |\alpha|^{2k} \approx h(x) e^{\frac{L}{3} f(x)} \quad (E5)$$

in the limit of large L , where we have introduced the function:

$$f(x) = (3-x)\log(3-x) - x\log x - (3-2x)\log(3-2x) + (2\log|\alpha|)x, \quad (\text{E6})$$

$$g(x) = 3\sqrt{\frac{3}{2\pi L}} \sqrt{\frac{1}{x(3-x)(3-2x)}}, \quad (\text{E7})$$

$$h(x) = \sqrt{\frac{3}{2\pi L}} \sqrt{\frac{(3-2x)^3}{x(3-x)^3}}. \quad (\text{E8})$$

We proceed by converting the summations over k in Eq. (E3) into continuous integrals over x and applying the saddle-point integration technique, in order to get to the final result:

$$\langle \alpha(t) | e^{i\pi j \hat{c}_{j+1} \hat{c}_j} | \alpha(t) \rangle = \alpha e^{i\frac{2\mu t}{h}} \frac{\int_0^{\frac{3}{2}} dx h(x) e^{\frac{L}{3} f(x)}}{\int_0^{\frac{3}{2}} dx g(x) e^{\frac{L}{3} f(x)}} \approx \frac{h(x^*)}{g(x^*)} = \frac{1}{3} \frac{(3-2x^*)^2}{3-x^*}, \quad (\text{E9})$$

where:

$$x^* = \frac{3}{2} \left(1 - \frac{1}{\sqrt{1+4|\alpha|^2}} \right) \quad (\text{E10})$$

satisfies $f'(x^*) = 0$. Plugging the expression of x^* into Eq. (E9), one recovers Eq. (21).

Appendix F: Entanglement entropy of the states $|\psi_{k,\pi}\rangle$

For the sake of convenience, we introduce the states:

$$|\psi_{k,q}\rangle = \frac{1}{\sqrt{\binom{L-k}{k}}} \frac{(\hat{\eta}_q^\dagger)^k}{k!} |0\rangle, \quad \text{with } \hat{\eta}_q^\dagger = \sum_{j=1}^L e^{iqj} \hat{c}_j^\dagger \hat{c}_{j+1}^\dagger. \quad (\text{F1})$$

Furthermore, we describe a general relation between the states $|\psi_{k,\pi}\rangle$ and the states $|\psi_{k,q}\rangle$. By introducing the unitary operator $\hat{U}_q = \prod_{j=1}^L e^{i\frac{\pi+q}{2} j \hat{n}_j}$, one can show that the following relation holds:

$$\hat{U}_q \hat{\eta}_\pi^\dagger \hat{U}_q^\dagger = e^{i\frac{\pi+q}{2}} \hat{\eta}_q^\dagger, \quad (\text{F2})$$

which in turn implies that:

$$|\psi_{k,q}\rangle = e^{-i\frac{\pi+q}{2}k} \hat{U}_q |\psi_{k,\pi}\rangle \quad (\text{F3})$$

Since the state $|\psi_{k,\pi}\rangle$ is related to the state $|\psi_{k,q}\rangle$ by a unitary transformation, we underline that the states $|\psi_{k,\pi}\rangle$ are eigenstates of \hat{H} if and only if the states $|\psi_{k,q}\rangle$ are eigenstates of $\hat{U}_q \hat{H} \hat{U}_q^\dagger$.

We start by evaluating the half-chain entanglement entropy for the states $|\psi_{k,0}\rangle$. We can distinguish among the configurations in which no pair is placed on the sites $\frac{L}{2}$ and $\frac{L}{2} + 1$ and the configurations in which this is instead the case:

$$\begin{aligned} |\psi_{k,0}\rangle = & \frac{1}{\sqrt{\binom{L-k}{k}}} \left[\sum_{n=\max\{0, \lceil \frac{N-L/2}{2} \rceil\}}^{\min\{\frac{N}{2}, \lfloor \frac{L/2}{2} \rfloor\}} \sum_{\substack{\{\vec{j}_{P,[1,\dots,\frac{L/2}]}\}^{(n)} \\ \{\vec{j}_{P,[\frac{L/2}+1,\dots,L]}\}^{(\frac{N}{2}-n)}}} \left| \vec{j}_{P,[1,\dots,\frac{L/2}]}\right\rangle \left| \vec{j}_{P,[\frac{L/2}+1,\dots,L]}\right\rangle \right] + \\ & + \sum_{l=\max\{0, \lceil \frac{N-L/2-1}{2} \rceil\}}^{\min\{\frac{N}{2}-1, \lfloor \frac{L/2-1}{2} \rfloor\}} \sum_{\substack{\{\vec{j}_{P,[1,\dots,\frac{L/2}-1]}\}^{(n)} \\ \{\vec{j}_{P,[\frac{L/2}+2,\dots,L]}\}^{(\frac{N}{2}-1-n)}}} \left| \vec{j}_{P,[1,\dots,\frac{L/2}-1]}; \bullet \right\rangle \left| \bullet; \vec{j}_{P,[\frac{L/2}+2,\dots,L]}\right\rangle \right], \quad (\text{F4}) \end{aligned}$$

where the symbol \bullet indicates an occupied site and the notation of the form $\left| \vec{j}_{P,[1,\dots,\frac{L/2}]}\right\rangle$ denote the equal-weight (with

unit weight, hence unnormalized) superposition of all possible distributions of n pairs over the sites $i = 1, \dots, \frac{L}{2}$. By

denoting as \mathcal{F}_R the set of Fock configurations on the right half of the chain, the expression of the partial density matrix

$$\rho_{k,0}^{(\frac{L}{2})} = \text{Tr}_{[\frac{L}{2}+1,\dots,L]}(|\psi_{k,0}\rangle\langle\psi_{k,0}|) \text{ takes then the form:}$$

$$\begin{aligned} \rho_{k,0}^{(\frac{L}{2})} &= \frac{1}{\binom{L-k}{k}} \sum_{k \in \mathcal{F}_R} \left[\sum_{l=\max\{0, \lceil \frac{N-L/2}{2} \rceil\}}^{\min\{\frac{N}{2}, \lfloor \frac{L/2}{2} \rfloor\}} \sum_{\{j_{P,[1,\dots,\frac{L}{2}]}\}^{(\vec{n})}} \sum_{\{l_{P,[1,\dots,\frac{L}{2}]}\}^{(\vec{n})}} \left| j_{P,[1,\dots,\frac{L}{2}]}^{(\vec{n})} \right\rangle \left\langle l_{P,[1,\dots,\frac{L}{2}]}^{(\vec{n})} \right| \times \\ &\quad \times \left\langle k \left| j_{P, [\frac{L}{2}+1,\dots,L]}^{(\vec{n})} \right\rangle \left\langle l_{P, [\frac{L}{2}+1,\dots,L]}^{(\vec{n})} \left| k \right\rangle + \right. \\ &\quad + \sum_{l=\max\{0, \lceil \frac{N-L/2-1}{2} \rceil\}}^{\min\{\frac{N}{2}-1, \lfloor \frac{L/2-1}{2} \rfloor\}} \sum_{\{j_{P,[1,\dots,\frac{L}{2}-1]}\}^{(\vec{n})}} \sum_{\{l_{P, [\frac{L}{2}+2,\dots,L]}\}^{(\vec{n})}} \left| j_{P,[1,\dots,\frac{L}{2}-1]}^{(\vec{n})}; \bullet \right\rangle \left\langle l_{P,[1,\dots,\frac{L}{2}-1]}^{(\vec{n})}; \bullet \right| \times \\ &\quad \times \left. \left\langle k \left| j_{P, [\frac{L}{2}+2,\dots,L]}^{(\frac{N}{2}-1-n)} \right\rangle \left\langle \bullet; l_{P, [\frac{L}{2}+2,\dots,L]}^{(\frac{N}{2}-1-n)} \left| k \right\rangle \right]. \right. \end{aligned}$$

For every configuration $k \in \mathcal{F}_R$ that results in a nonvanishing scalar product in the above expression, one obtains the unnormalized equal-weight superposition with unit weight of all configurations in the left half of the system that are com-

patible with it. After normalizing the latter and counting all configurations $k \in \mathcal{F}_R$ that give a nonzero contribution, one obtains:

$$\begin{aligned} \rho_{k,0}^{(\frac{L}{2})} &= \sum_{l=\max\{0, \lceil \frac{N-L/2}{2} \rceil\}}^{\min\{\frac{N}{2}, \lfloor \frac{L/2}{2} \rfloor\}} \left| \varphi_l^{[1,\dots,\frac{L}{2}]} \right\rangle \left\langle \varphi_l^{[1,\dots,\frac{L}{2}]} \right| \frac{\binom{\frac{L}{2}-\frac{N}{2}+l}{\frac{L}{2}-l} \binom{\frac{L}{2}-l}{l}}{\binom{L-\frac{N}{2}}{\frac{N}{2}}} + \\ &\quad + \sum_{l=\max\{0, \lceil \frac{N-L/2-1}{2} \rceil\}}^{\min\{\frac{N}{2}-1, \lfloor \frac{L/2-1}{2} \rfloor\}} \left| \varphi_l^{[1,\dots,\frac{L}{2}-1]} \right\rangle \left\langle \bullet; \varphi_l^{[1,\dots,\frac{L}{2}-1]} \right| \frac{\binom{\frac{L}{2}-\frac{N}{2}+l}{\frac{L}{2}-l-1} \binom{\frac{L}{2}-1-l}{l}}{\binom{L-\frac{N}{2}}{\frac{N}{2}}}, \end{aligned} \quad (\text{F5})$$

where $\left| \varphi_l^{[1,\dots,s]} \right\rangle$ denotes the normalized equal-weight superposition of all Fock states with l pairs distributed over s lattice sites and $|\bullet\rangle$ indicates the occupation of site $\frac{L}{2}$. The eigenvalues λ_s of the reduced density matrix $\rho_{k,0}$ can be read off directly Eq. (F5) as the coefficients of each term of the summations in Eq. (F5), and the second Renyi entropy can be computed accordingly as $S_{\frac{L}{2},k,0} = -\log(\sum_s \lambda_s^2)$.

We now proceed to show that the half-chain entanglement entropy of the states $|\psi_{k,\pi}\rangle$ defined in Eq. (2) equals the one of the states $|\psi_{k,0}\rangle$ introduced via Eq. (F3), thus showing that the subvolume entanglement scaling law holds for both towers of states. To this end, we recall the previously defined unitary operator $\hat{U}_0 = \prod_{j=1}^L e^{i\frac{\pi}{2}j\hat{n}_j}$. After using Eq. (F3) and notic-

ing that \hat{U}_0 factorizes as $\hat{U}_0 = \hat{U}_{0,[1,\frac{L}{2}]} \hat{U}_{0, [\frac{L}{2}+1,L]}$, where $\hat{U}_{0,[1,\frac{L}{2}]} = \prod_{j=1}^{\frac{L}{2}} e^{i\frac{\pi}{2}j\hat{n}_j}$ and $\hat{U}_{0, [\frac{L}{2}+1,L]} = \prod_{j=\frac{L}{2}+1}^L e^{i\frac{\pi}{2}j\hat{n}_j}$, the half-chain reduced density matrix for a generic state $|\psi_{k,\pi}\rangle$ can then be expressed as:

$$\rho_{k,\pi}^{(\frac{L}{2})} = \frac{1}{(k!)^2 \binom{L-k}{k}} \hat{U}_{0,[1,\frac{L}{2}]} \quad (\text{F6})$$

$$\cdot \text{Tr}_{[\frac{L}{2}+1,\dots,L]} \left[\hat{U}_{0, [\frac{L}{2}+1,L]} (\hat{\eta}_0^\dagger)^k |0\rangle \langle 0| (\hat{\eta}_0)^k \hat{U}_{0, [\frac{L}{2}+1,L]}^\dagger \right] \hat{U}_{0,[1,\frac{L}{2}]}^\dagger.$$

By making use of the cyclic invariance property of the trace, the reduced density matrix for the states $|\psi_{k,\pi}\rangle$ is manifestly shown to be related to the corresponding quantity for the states $|\psi_{k,0}\rangle$ via a similarity transformation implemented by a uni-

tary operator, i.e.:

$$\rho_{k,\pi}^{(\frac{L}{2})} = \hat{U}_{0,[1,\frac{L}{2}]} \text{Tr}_{[\frac{L}{2}+1,\dots,L]} [|\psi_{k,0}\rangle \langle \psi_{k,0}|] \hat{U}_{0,[1,\frac{L}{2}]}^\dagger, \quad (\text{F7})$$

which leaves the entanglement entropy unaffected.

We are now in a position to estimate the large- L scaling of the second Renyi entropy of the states $|\psi_{k,\pi}\rangle$ analytically in the case $k = L/3$, designed to ensure that the binomial coefficients in the numerator of the combinatorial coefficient in the first row of Eq. (F5) are peaked around the same value of $l = L/6 = O(L)$. After introducing the rescaled variable $x = 6l/L$, one obtains by means of the Stirling approximation

the asymptotic behaviors:

$$\frac{\binom{\frac{L}{2} - \frac{N}{2} + l}{\frac{N}{2} - l} \binom{\frac{L}{2} - l}{l}}{\binom{L - \frac{N}{2}}{\frac{N}{2}}} \approx g(x) e^{\frac{L}{6} f(x)}, \quad (\text{F8})$$

$$\frac{\binom{\frac{L}{2} - \frac{N}{2} + l}{\frac{N}{2} - l - 1} \binom{\frac{L}{2} - 1 - l}{l}}{\binom{L - \frac{N}{2}}{\frac{N}{2}}} \approx h(x) e^{\frac{L}{6} f(x)}, \quad (\text{F9})$$

where the large L limit has been taken and we have introduced the functions:

$$f(x) = (1+x) \log(1+x) + (3-x) \log(3-x) - (2-x) \log(2-x) - (2x-1) \log(2x-1) - x \log x - (3-2x) \log(3-2x) - 4 \log 2, \quad (\text{F10})$$

$$g(x) = \sqrt{\frac{3}{\pi L} \frac{(1+x)(3-x)}{x(2-x)(2x-1)(3-2x)}}, \quad (\text{F11})$$

$$h(x) = \frac{(2-x)(3-2x)}{(3-x)(2x-1)} g(x). \quad (\text{F12})$$

Armed with these expressions, we proceed to evaluate the argument of Eq. (23) by converting the discrete sums over l into continuous integrals over x and applying the saddle-point integration technique:

$$\begin{aligned} & \sum_{l=\max\{0, \lceil \frac{N-L/2}{2} \rceil\}}^{\min\{\frac{N}{2}, \lfloor \frac{L/2}{2} \rfloor\}} \left(\frac{\binom{\frac{L}{2} - \frac{N}{2} + l}{\frac{N}{2} - l} \binom{\frac{L}{2} - l}{l} \right)^2 + \sum_{l=\max\{0, \lceil \frac{N-L/2-1}{2} \rceil\}}^{\min\{\frac{N}{2}-1, \lfloor \frac{L/2-1}{2} \rfloor\}} \left(\frac{\binom{\frac{L}{2} - \frac{N}{2} + l}{\frac{N}{2} - l - 1} \binom{\frac{L}{2} - 1 - l}{l} \right)^2 \approx \\ & \approx \frac{L}{6} \left(\int_{\frac{1}{2}}^{\frac{3}{2}} dx g^2(x) e^{\frac{L}{3} f(x)} + \int_{\frac{1}{2}}^{\frac{3}{2}} dx h^2(x) e^{\frac{L}{3} f(x)} \right) \approx \frac{L}{6} e^{\frac{L}{3} f(x^*)} \sqrt{\frac{6\pi}{L|f''(x^*)|}} (g^2(x^*) + h^2(x^*)), \end{aligned} \quad (\text{F13})$$

where $x^* = 1$ satisfies $f'(x^*) = 0$ and $f''(x^*) < 0$. After a straightforward substitution of the numerical value of x^* in Eq. (F13), one gets the result $\frac{5}{\sqrt{6\pi L}}$, which in turns gives the logarithmic scaling in Eq. (24) once plugged into Eq. (23).

As a final consistency check, we verify that the large L asymptotic behavior of the eigenvalues of the half-chain reduced density matrix $\rho_{k,\pi}^{(\frac{L}{2})}$ preserves the normalization condition that they are subject to. Specifically, we evaluate $\text{Tr} \left[\rho_{k,\pi}^{(\frac{L}{2})} \right]$, namely:

$$\begin{aligned} & \sum_{l=\max\{0, \lceil \frac{N-L/2}{2} \rceil\}}^{\min\{\frac{N}{2}, \lfloor \frac{L/2}{2} \rfloor\}} \frac{\binom{\frac{L}{2} - \frac{N}{2} + l}{\frac{N}{2} - l} \binom{\frac{L}{2} - l}{l}}{\binom{L - \frac{N}{2}}{\frac{N}{2}}} + \sum_{l=\max\{0, \lceil \frac{N-L/2-1}{2} \rceil\}}^{\min\{\frac{N}{2}-1, \lfloor \frac{L/2-1}{2} \rfloor\}} \frac{\binom{\frac{L}{2} - \frac{N}{2} + l}{\frac{N}{2} - l - 1} \binom{\frac{L}{2} - 1 - l}{l}}{\binom{L - \frac{N}{2}}{\frac{N}{2}}} \approx \\ & \approx \frac{L}{6} \left(\int_{\frac{1}{2}}^{\frac{3}{2}} dx g(x) e^{\frac{L}{6} f(x)} + \int_{\frac{1}{2}}^{\frac{3}{2}} dx h(x) e^{\frac{L}{6} f(x)} \right) \approx \frac{L}{6} e^{\frac{L}{6} f(x^*)} \sqrt{\frac{12\pi}{L|f''(x^*)|}} (g(x^*) + h(x^*)) = 1, \end{aligned} \quad (\text{F14})$$

consistently with the expected result.

Appendix G: Some additional results on multimer scars

In Sec. V we have introduced the Hamiltonian \hat{H}_J as a frustration-free positive Hamiltonian of the form $J \sum_j \hat{L}_j^{\dagger(M)} \hat{L}_j^{(M)}$. The explicit expression of $\hat{L}_j^{(M)}$ reads

$$\begin{aligned} \hat{L}_j^{(M)} &= \prod_{l=0}^{M-1} \hat{n}_{j+l} - \prod_{l=0}^{M-1} \hat{n}_{j+l+1} - (-1)^M \hat{c}_j^\dagger \left(\prod_{l=1}^{M-1} \hat{n}_{j+l} \right) \hat{c}_{j+M} + (-1)^M \hat{c}_{j+M}^\dagger \left(\prod_{l=1}^{M-1} \hat{n}_{j+l} \right) \hat{c}_j = \\ &= \prod_{l=0}^{M-1} \hat{n}_{j+l} - \prod_{l=0}^{M-1} \hat{n}_{j+l+1} + \hat{M}_j^\dagger \hat{M}_{j+1} - \hat{M}_j^\dagger \hat{M}_j \end{aligned} \quad (\text{G1})$$

-
- [1] J. M. Deutsch, *Phys. Rev. A* **43**, 2046 (1991).
[2] M. Srednicki, *Phys. Rev. E* **50**, 888 (1994).
[3] M. Rigol, V. Dunjko, and M. Olshanii, *Nature* **452**, 854 (2008).
[4] J. M. Deutsch, *Reports on Progress in Physics* **81**, 082001 (2018).
[5] L. Vidmar and M. Rigol, *Journal of Statistical Mechanics: Theory and Experiment* **2016**, 064007 (2016).
[6] F. H. L. Essler and M. Fagotti, *Journal of Statistical Mechanics: Theory and Experiment* **2016**, 064002 (2016).
[7] M. Rigol, V. Dunjko, V. Yurovsky, and M. Olshanii, *Phys. Rev. Lett.* **98**, 050405 (2007).
[8] P. Calabrese, F. H. L. Essler, and M. Fagotti, *Phys. Rev. Lett.* **106**, 227203 (2011).
[9] B. Pozsgay, *Journal of Statistical Mechanics: Theory and Experiment* **2013**, P07003 (2013).
[10] M. Fagotti and F. H. L. Essler, *Journal of Statistical Mechanics: Theory and Experiment* **2013**, P07012 (2013).
[11] T. M. Wright, M. Rigol, M. J. Davis, and K. V. Kheruntsyan, *Phys. Rev. Lett.* **113**, 050601 (2014).
[12] E. Ilievski, J. De Nardis, B. Wouters, J.-S. Caux, F. H. L. Essler, and T. Prosen, *Phys. Rev. Lett.* **115**, 157201 (2015).
[13] D. Basko, I. Aleiner, and B. Altshuler, *Annals of Physics* **321**, 1126 (2006).
[14] J. H. Bardarson, F. Pollmann, and J. E. Moore, *Phys. Rev. Lett.* **109**, 017202 (2012).
[15] M. Serbyn, Z. Papić, and D. A. Abanin, *Phys. Rev. Lett.* **110**, 260601 (2013).
[16] M. Serbyn, Z. Papić, and D. A. Abanin, *Phys. Rev. Lett.* **111**, 127201 (2013).
[17] D. A. Huse, R. Nandkishore, and V. Oganesyan, *Phys. Rev. B* **90**, 174202 (2014).
[18] D. J. Luitz, N. Laflorencie, and F. Alet, *Phys. Rev. B* **91**, 081103 (2015).
[19] A. Chandran, I. H. Kim, G. Vidal, and D. A. Abanin, *Phys. Rev. B* **91**, 085425 (2015).
[20] V. Ros, M. Müller, and A. Scardicchio, *Nuclear Physics B* **891**, 420 (2015).
[21] R. Nandkishore and D. A. Huse, *Annual Review of Condensed Matter Physics* **6**, 15 (2015).
[22] H. Bernien, S. Schwartz, A. Keesling, H. Levine, A. Omran, H. Pichler, S. Choi, A. S. Zibrov, M. Endres, M. Greiner, et al., *Nature* **551**, 579 (2017).
[23] C. J. Turner, A. A. Michailidis, D. A. Abanin, M. Serbyn, and Z. Papić, *Nature Physics* **14**, 745 (2018).
[24] S. Moudgalya, B. A. Bernevig, and N. Regnault, *Reports on Progress in Physics* **85**, 086501 (2022).
[25] Z. Papić, arXiv preprint arXiv:2108.03460 (2021), <https://doi.org/10.48550/arXiv.2108.03460>.
[26] A. Chandran, T. Iadecola, V. Khemani, and R. Moessner, arXiv (2022), <https://doi.org/10.48550/ARXIV.2206.11528>.
[27] C. J. Turner, A. A. Michailidis, D. A. Abanin, M. Serbyn, and Z. Papić, *Phys. Rev. B* **98**, 155134 (2018).
[28] T. Iadecola, M. Schechter, and S. Xu, *Phys. Rev. B* **100**, 184312 (2019).
[29] S. Choi, C. J. Turner, H. Pichler, W. W. Ho, A. A. Michailidis, Z. Papić, M. Serbyn, M. D. Lukin, and D. A. Abanin, *Phys. Rev. Lett.* **122**, 220603 (2019).
[30] C.-J. Lin and O. I. Motrunich, *Phys. Rev. Lett.* **122**, 173401 (2019).
[31] C.-J. Lin, V. Calvera, and T. H. Hsieh, *Phys. Rev. B* **101**, 220304 (2020).
[32] G.-X. Su, H. Sun, A. Hudomal, J.-Y. Desaulles, Z.-Y. Zhou, B. Yang, J. C. Halimeh, Z.-S. Yuan, Z. Papić, and J.-W. Pan, arXiv (2022), <https://doi.org/10.48550/arXiv.2201.00821>.
[33] J.-Y. Desaulles, D. Banerjee, A. Hudomal, Z. Papić, A. Sen, and J. C. Halimeh, arXiv (2022), <https://doi.org/10.48550/arXiv.2203.08830>.
[34] J.-Y. Desaulles, A. Hudomal, D. Banerjee, A. Sen, Z. Papić, and J. C. Halimeh, arXiv (2022), <https://doi.org/10.48550/arXiv.2204.01745>.
[35] S. Moudgalya, S. Rachel, B. A. Bernevig, and N. Regnault, *Phys. Rev. B* **98**, 235155 (2018).
[36] S. Moudgalya, N. Regnault, and B. A. Bernevig, *Phys. Rev. B* **98**, 235156 (2018).
[37] S. Moudgalya, E. O'Brien, B. A. Bernevig, P. Fendley, and N. Regnault, *Phys. Rev. B* **102**, 085120 (2020).
[38] S. Chattopadhyay, H. Pichler, M. D. Lukin, and W. W. Ho, *Phys. Rev. B* **101**, 174308 (2020).
[39] D. K. Mark, C.-J. Lin, and O. I. Motrunich, *Phys. Rev. B* **101**, 195131 (2020).
[40] N. Shiraishi and T. Mori, *Phys. Rev. Lett.* **119**, 030601 (2017).
[41] T. Iadecola and M. Schechter, *Phys. Rev. B* **101**, 024306 (2020).
[42] C. M. Langlett and S. Xu, *Phys. Rev. B* **103**, L220304 (2021).
[43] N. Shibata, N. Yoshioka, and H. Katsura, *Phys. Rev. Lett.* **124**, 180604 (2020).
[44] S. Moudgalya, N. Regnault, and B. A. Bernevig, *Phys. Rev. B* **102**, 085140 (2020).
[45] D. K. Mark and O. I. Motrunich, *Phys. Rev. B* **102**, 075132 (2020).
[46] J.-Y. Desaulles, A. Hudomal, C. J. Turner, and Z. Papić, *Phys.*

- Rev. Lett.* **126**, 210601 (2021).
- [47] S. Moudgalya, B. A. Bernevig, and N. Regnault, *Phys. Rev. B* **102**, 195150 (2020).
- [48] B. Mukherjee, S. Nandy, A. Sen, D. Sen, and K. Sengupta, *Phys. Rev. B* **101**, 245107 (2020).
- [49] H. Zhao, J. Vovrosh, F. Mintert, and J. Knolle, *Phys. Rev. Lett.* **124**, 160604 (2020).
- [50] K. Mizuta, K. Takasan, and N. Kawakami, *Phys. Rev. Research* **2**, 033284 (2020).
- [51] S. Sugiura, T. Kuwahara, and K. Saito, *Phys. Rev. Research* **3**, L012010 (2021).
- [52] D. Banerjee and A. Sen, *Phys. Rev. Lett.* **126**, 220601 (2021).
- [53] J. C. Halimeh, L. Barbiero, P. Hauke, F. Grusdt, and A. Bohrdt, (2022), <https://doi.org/10.48550/ARXIV.2203.08828>.
- [54] A. S. Aramthottil, U. Bhattacharya, D. González-Cuadra, M. Lewenstein, L. Barbiero, and J. Zakrzewski, *Phys. Rev. B* **106**, L041101 (2022).
- [55] P. A. McClarty, M. Haque, A. Sen, and J. Richter, *Phys. Rev. B* **102**, 224303 (2020).
- [56] Y. Kuno, T. Mizoguchi, and Y. Hatsugai, *Phys. Rev. B* **102**, 241115 (2020).
- [57] K. Lee, R. Melendrez, A. Pal, and H. J. Changlani, *Phys. Rev. B* **101**, 241111 (2020).
- [58] K. Lee, A. Pal, and H. J. Changlani, *Phys. Rev. B* **103**, 235133 (2021).
- [59] C. N. Yang, *Phys. Rev. Lett.* **63**, 2144 (1989).
- [60] O. Vafek, N. Regnault, and B. A. Bernevig, *SciPost Phys.* **3**, 043 (2017).
- [61] M. Schechter and T. Iadecola, *Phys. Rev. Lett.* **123**, 147201 (2019).
- [62] K. Pakrouski, P. N. Pallegar, F. K. Popov, and I. R. Klebanov, *Phys. Rev. Lett.* **125**, 230602 (2020).
- [63] M. Nakagawa, H. Katsura, and M. Ueda, *arXiv* (2022), <https://doi.org/10.48550/arXiv.2205.07235>.
- [64] H. Yoshida and H. Katsura, *Phys. Rev. B* **105**, 024520 (2022).
- [65] A. M. Alhambra, A. Anshu, and H. Wilming, *Phys. Rev. B* **101**, 205107 (2020).
- [66] J. Ren, C. Liang, and C. Fang, *Phys. Rev. Lett.* **126**, 120604 (2021).
- [67] N. O’Dea, F. Burnell, A. Chandran, and V. Khemani, *Phys. Rev. Research* **2**, 043305 (2020).
- [68] R. Z. Bariev, *Journal of Physics A: Mathematical and General* **24**, L549 (1991).
- [69] R. W. Chhajlany, P. R. Grzybowski, J. Stasińska, M. Lewenstein, and O. Dutta, *Phys. Rev. Lett.* **116**, 225303 (2016).
- [70] J. Ruhman and E. Altman, *Phys. Rev. B* **96**, 085133 (2017).
- [71] L. Gotta, L. Mazza, P. Simon, and G. Roux, *Phys. Rev. Lett.* **126**, 206805 (2021).
- [72] L. Gotta, L. Mazza, P. Simon, and G. Roux, *Phys. Rev. B* **104**, 094521 (2021).
- [73] L. Gotta, L. Mazza, P. Simon, and G. Roux, *Phys. Rev. B* **105**, 134512 (2022).
- [74] L. P. Pitaevskii and S. Stringari, *Bose-Einstein Condensation* (Oxford University Press, 2003).
- [75] P. Weinberg and M. Bukov, *SciPost Phys.* **2**, 003 (2017).
- [76] P. Weinberg and M. Bukov, *SciPost Phys.* **7**, 20 (2019).
- [77] V. Oganesyan and D. A. Huse, *Phys. Rev. B* **75**, 155111 (2007).
- [78] Y. Y. Atas, E. Bogomolny, O. Giraud, and G. Roux, *Phys. Rev. Lett.* **110**, 084101 (2013).
- [79] L. Mazza, F. Iemini, M. Dalmonte, and C. Mora, *Phys. Rev. B* **98**, 201109 (2018).
- [80] K. Tamura and H. Katsura, *arXiv* (2022), <https://doi.org/10.48550/arXiv.2207.06040>.